Double Charmonia Production at LHCb

A V Luchinsky

Institute for High Energy Physics, Protvino, Russia

E-mail: alexey.luchinsky@ihep.ru

Abstract. In this note next-to-leading order corrections to double charmonium production at LHCb are considered. It is shown that real gluon emission leads to significant change of the cross sections of considered processes. For example, forbidden at leading order production of C-odd state $\chi_c J/\psi$ is possible at NLO. Distributions over various kinematical variables are analyzed and the question of separating contributions of different mechanisms (direct $J/\psi J/\psi$ production, radiative feed-down from $\chi_c J/\psi$, double parton scattering) is considered.

1. Introduction

Presented article is devoted to theoretical study of real gluon emission effects to double charmonia production at LHC.

Charmonium production in high energy hadronic interaction was studied in details both theoretically and in experiment. In the case of single charmonium production the main theoretical approaches include:

- Leading order (LO) processes $gg \to \mathcal{Q}$. In the collinear gluon approximation this approach cannot describe final meson's transverse momentum distribution. In addition, due to charge parity conservation production of C-odd states (e.g. J/ψ) is forbidden.
- k_T factorization [1]. In this model transverse momentum dependence of initial gluons' structure functions is taken into account, so p_T distributions can be described. Charge parity selection rules, however, still hold and J/ψ meson cannot be produced.
- Next-to-Leading-Order (NLO) processes $gg \to \mathcal{Q}g$. Due to the presence of additional final gluon all mentioned above problems can be solved. This approach was used, for example, in papers [2, 3] and good agreement with experiment was observed.

Recently the era of double charmonium production began [4–7]. It is clear, that in this case the same theoretical methods can be used and they have the same problems. For example, in LO collinear gluon approximation [8–10] one cannot describe distribution over the transverse momentum of the pair. Due to charge parity conservation C-odd final states (e.g. $J/\psi\chi_{cJ}$, $J/\psi\eta_c$, etc.) cannot be produced. As in the case of single charmonium production all these problems can be solved if one consider NLO processes $gg \to \mathcal{Q}_1\mathcal{Q}_2 g$.

Next to leading order corrections to double charmonium production in high energy hadronic interactions were studied already theoretically [11–13]. In these articles, however, only production of S-wave charmonia states was considered and theoretical predictions were made only for LHC experiment at $\sqrt{s} = 7\,\text{TeV}$. In the presented article we are going to consider $\sqrt{s} = 13\,\text{TeV}$ experiment and study also production of P-wave charmonium states χ_{cJ}.

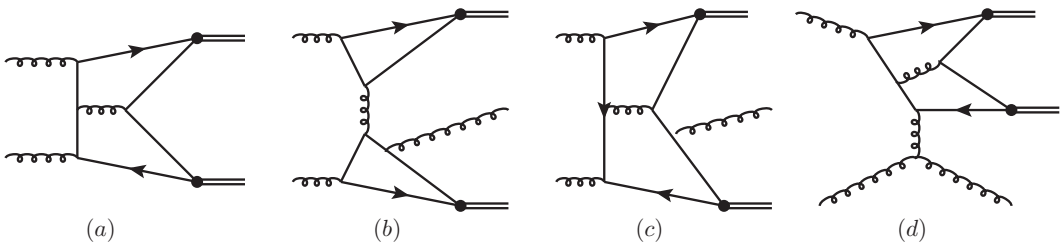

Figure 1. Typical Feynman diagrams of double charmonium production in gluon interaction at LO (a) and NLO* (b,c,d)

The rest of the paper is organized as follows. In the next section we study partonic cross sections of $gg \to \psi\psi g$ and $gg \to \psi\chi_{cJ} g$ processes. In section III hadronic reactions are considered. The last section is reserved for brief discussion.

2. Partonic Processes

In our paper we will use Non-relativistic quantum (NRQCD) [14, 15] and restrict ourselves to leading order in relative quarks' velocity colour-singlet (CS) approximation. Under these assumptions the matrix element of the considered process can be factorized into short distance and long distance parts. The first is easily calculated in perturbation theory, while for the latter one, that describes quark-antiquark pair hadronization into physical meson, some nonperturbative methods should be used. We prefer to determine the long distance matrix elements from experimental widths of the corresponding J/ψ and χ_c meson decays.

Let us first discuss briefly leading order contribution to $gg \to J/\psi J/\psi$ reaction. In total there are 72 Feynman diagrams that can contribute to this process with the typical one shown in Fig.1(a). Few comments should be made. First of all, since each quark carries one half of meson's momentum, significant suppression is present and the corresponding cross section falls rapidly with the increase of the partonic energy $\sqrt{\hat{s}}$. In addition, due to back-to-back kinematics, in this process neither $p_T^{\rm pair}$ nor azimuthal distribution can be described. Finally, no C-odd final states (e.g. $J/\psi\chi_c$) can be produced due to charge parity conservation. Since experimentally both these distributions and final states are observed it is clear that LO description is unsatisfactory and NLO contributions should be taken into account.

There are two significant ingredients that should be taken into account at NLO. The first one is 1-loop diagrams. It is clear, however that for these diagrams all mentioned above drawbacks still hold: due to back-to-back kinematics some important distributions cannot be described and charge parity selection rules are still present. For this reason we will not consider 1-loop corrections in the following. In addition at NLO there are diagrams with real gluon emission, that can both generate transverse momentum and azimuthal distributions and allow the production of C-odd final state. Typical diagrams of this type are shown in Fig.1(b-d). In total there are 438 such diagrams, but charge parity conservation leads to cancellation of some sets of these diagrams. It is important to notice that for different final states ($J/\psi J/\psi$ or $J/\psi\chi_c$) contributions of different diagrams cancel.

Let us consider first direct production of $J/\psi J/\psi$ pair at NLO. First of all, it is clear that colour-singlet vector meson cannot couple to two (possible virtual) gluons, so 106 diagrams similar to those shown in Fig.1(b) do not contribute. Next, at the leading order in relative quarks' momentum all final state radiation diagrams (see Fig.1c) give finite result. Thus, the only divergent diagrams are initial state radiation (ISR), like the one shown in Fig.1(d). This divergence can be compensated by 1-loop corrections to hadron distribution functions, but we chose to put a cut-off on the transverse momentum of final charmonium pair $p_T^{\rm pair} > \Delta$. It is

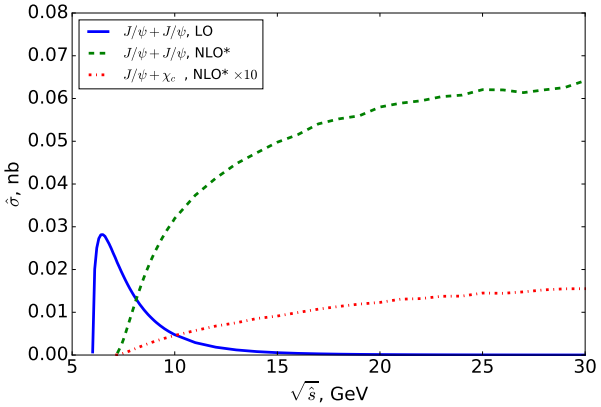

Figure 2. Partonic cross sections of LO $J/\psi J/\psi$ (solid line), NLO $J/\psi J/\psi$ (dashed line) and $J/\psi\chi_c$ (dotted line) reactions

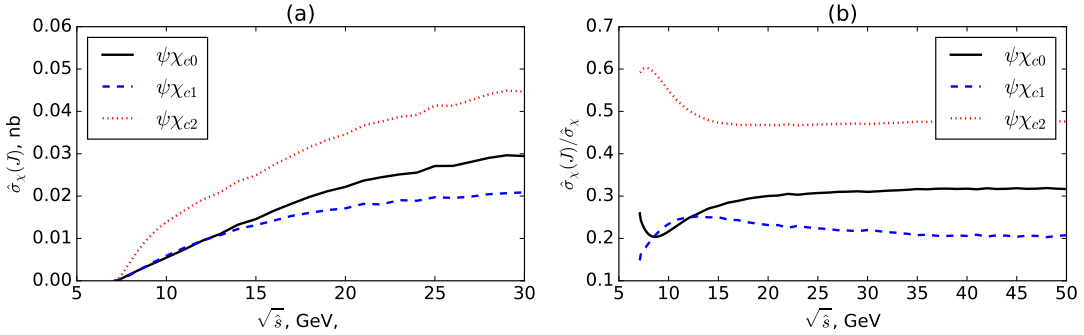

Figure 3. Partonic cross sections $\hat{\sigma}_\chi(J) = \hat{\sigma}(gg \to J/\psi\chi_{cJ}g)$. The value $\hat{\sigma}_\chi$ in the right figure stands for total partonic cross section $\sum_J \hat{\sigma}_\chi(J)$

also interesting to note that contributions of symmetric color structure d_{abc} cancel and only antisymmetric one f_{abc} is left. These cancellation can be explained by assigning negative and positive charge parities to f_{abc} and d_{abc} respectively.

The situation is completely different in the case of $J/\psi\chi_c$ final state. First of all, χ_c meson can couple to gluon pair, so only half of the processes shown in Fig.1(b) diagrams cancel. Since we have to keep some quarks' relative momentum to produce P-wave meson state some of Final State Radiation (FSR) diagrams are collinearly divergent. This divergence can be absorbed if one takes into account contributions of colour-octet components, but we prefer to regularize them by imposing a restriction $k_g p_\chi > \Delta^2$. As for shown in Fig.1(d) ISR diagrams, there contribution completely cancel due to charge parity conservation in $gg \to J/\psi\chi_c$ block. Finally, our calculations show that in the case of $J/\psi\chi_c$ final state only symmetric colour structure d_{abc} is left.

To summarize, we can see, that by changing the final state one can switch on and off different sets of the underlying Feynman diagrams and change the overall colour structure of the corresponding amplitude.

In Fig.2 we show partonic cross sections of $J/\psi J/\psi$ at LO, NLO, and feed-down from radiative $J/\psi\chi_c$ decays. It is clearly seen, that the leading order cross section falls rapidly with the increase of partonic energy, while NLO ones grow. It should be also noted that NLO corrections to double J/ψ production cross section are comparable with LO. In Fig.3 partonic energy dependence of

Cut	$J/\psi + J/\psi$, LO	$J/\psi + J/\psi$, NLO*	$J/\psi + \chi_{cJ}$, f.-d.	DPS
$\Delta = 1$ GeV	1.29 ± 0.02 nb	4.47 ± 0.79 nb	10.8 ± 1.54 pb	6.2 ± 2.1 nb
$\Delta = 3$ GeV		1.68 ± 0.33 nb	2.41 ± 0.4 pb	4.0 ± 0.6 nb

Table 1. Hadronic cross sections in the LHCb acceptance at $\sqrt{s} = 13$ TeV.

$J/\psi\chi_{cJ}$ partonic cross sections is shown. From the right panel of this figure it is clear that in low energy region cross sections of scalar and tensor meson production increase, while in the case of axial meson the situation is infrared safe. Possible explanation of this behaviour is that due to Landau-Yang theorem axial meson cannot couple to two massless gluons. The same situation was observed in the case of single charmonium production [2, 3].

3. Hadronic Results

Let us now discuss theoretical predictions for double charmonium production in hadronic experiments. In the following results for LHCb detector (with the cut $2 < y < 4.5$ set on rapidity of final charmonia) are presented.

It turns out, that there are two possible mechanisms that can contribute to the considered process. The first one is usual single parton scattering (SPS), when cross section of the hadronic process is written as convolution of the discussed in previous section partonic cross sections and gluons' distribution functions (in the following CT10, CT14 parametrizations [16, 17] are used):

$$d\sigma = \int_0^1 dx_1 dx_2 f_g(x_1, \mu) f_g(x_2, \mu) d\hat{\sigma}(\mu). \quad (1)$$

It is important to note that both partonic distribution functions and strong coupling constant in partonic cross section depend on scale parameter. In order to study dependence of final results on scale choice we vary the value of this parameter from $\mu/2$ to μ, where $\mu^2 = 16\, m_c^2 + (p_T^{\psi})^2 + (p_T^{\chi})^2$ is the transverse mass of the pair. The other possible mechanism is so called double parton scattering (DPS), where it is assumed that final charmonia are produced in two almost independent partonic reactions. In this case the formula for hadronic cross section is surprisingly simple:

$$\sigma = \frac{1}{2}\frac{\sigma_{\psi}\sigma_{\psi}}{\sigma_{\text{eff}}}, \quad (2)$$

where $\sigma_{\psi} = 15.3 \pm 1\, \mu b$ and $\sigma_{\text{eff}} = 18 \pm 1.8$ mb are the cross section of single J/ψ production at LHCb [18] and the effective cross section [19]respectively. Our theoretical predictions for hadronic cross sections are shown in table 1. It is worth noting that in paper [12] the value $\sigma_{\text{eff}} = 8.2 \pm 2.0 \pm 2.9$ mb was proposed. It is clear, that with this value of the effective cross section the contribution of DPS mechanism is approximately doubled.

From presented table it is evident that contributions of different mechanisms are comparable to each other. To separate them one can study distributions over different kinematical variables. In Fig. 4, for example, we show distributions over invariant mass and transverse momentum of $J/\psi J/\psi$ pair with the cut-off parameter $\Delta = 1$ GeV (it turns out that the form of these distributions only slightly depends on Δ). It can be seen that in both cases distributions of different mechanisms are nearly the same. The situation is completely different for distribution over azimuthal asymmetry $\Delta\phi = |\phi_1 - \phi_2|$. From Fig. 5 it is clear that in this case the distribution form for different mechanisms are different and strongly depends on the choice of the cut-off parameter.

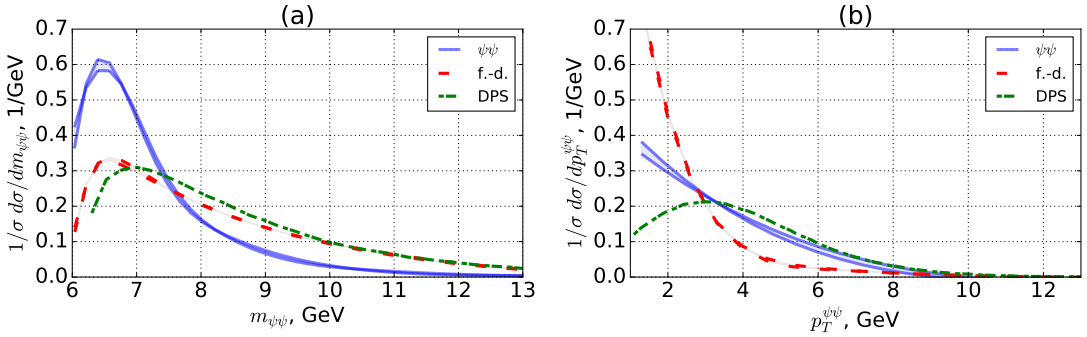

Figure 4. Distributions over invariant mass (left panel) and transverse momentum (right panel) of the charmonium pair

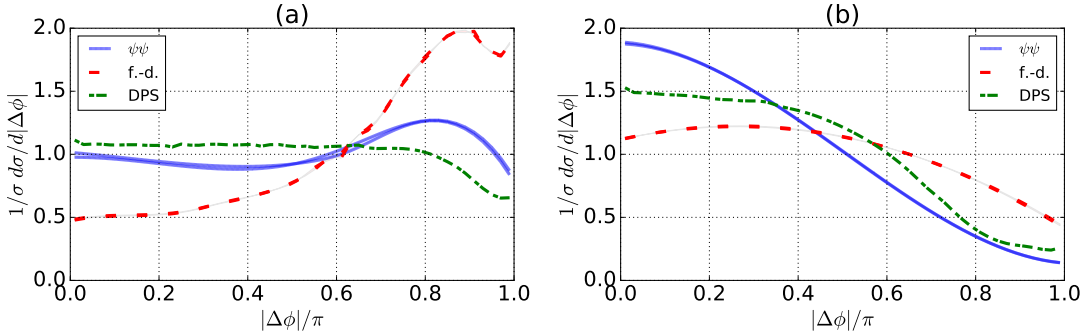

Figure 5. Distribution over $\Delta\phi = |\phi_1 - \phi_2|$ for $\Delta = 1\,\text{GeV}$ (left panel) and $\Delta = 3\,\text{GeV}$ (right panel)

We have analyzed also distributions over other kinematical variables. To be clear but concise it is desirable to quantitize in some way difference between them. In order to do this one can use, for example, the parameter connected with the Pearson correlator:

$$A_a^{(i,j)} \quad = \quad 1 - \left\langle \frac{d\sigma_i}{da}, \frac{d\sigma_j}{da} \right\rangle, \tag{3}$$

where a is some kinematical variable ($m_{\psi\psi}$, $p_T^{\psi\psi}$ are invariant mass and trasverse momentum of final charmonium pair, $\Delta\phi = \phi_1 - \phi_2$, $\Delta y = y_1 - y_2$, and $A^T = (p_T^{\psi 1} - p_T^{\psi 2})/(p_T^{\psi 1} + p_T^{\psi 2})$ are azimuthal, rapidity, and transsvers momentum assymetries, $y_{J/\psi}$ is the rapidity of single charmonium), and i, j stand for different subprocesses. From table 2, where the values of this parameter are shown, it is clear, for example, that $y_{J/\psi}$ distribution is post suitable for separation of direct $J/\psi J/\psi$ and feed-down from $J/\psi\chi_c$ signals.

4. Conclusion

Let me summarize the brief results of the talk.

It was shown, that in contrast to leading order next-to-leading-order approach is satisfactory for description of double charmonium production at LHC. Our calculations show that in the case of $J/\psi J/\psi$ final state NLO contributions are comparable or even larger then LO ones. It also turns out that production mechanisms on the partonic level depend strongly on the final

	Combination	$m_{\psi\psi}$	$p_T^{\psi\psi}$	$\lvert\Delta\phi\rvert$	Δy	A_T	$y_{J/\psi}$
$\Delta = 1\,\text{GeV}$	$J/\psi + J/\psi$ vs $J/\psi + \chi_c$	0.10	0.02	0.26	0.10	0.01	**0.54**
	$J/\psi + J/\psi$ vs DPS	0.21	0.21	**0.79**	0.09	0.00	0.55
	$J/\psi + \chi_c$ vs DPS	0.03	**0.34**	0.26	0.01	0.01	0.01
$\Delta = 3\,\text{GeV}$	$J/\psi + J/\psi$ vs $J/\psi + \chi_c$	0.07	0.01	0.14	0.03	0.05	0.16
	$J/\psi + J/\psi$ vs DPS	**0.20**	0.02	0.04	0.11	0.00	0.15
	$J/\psi + \chi_c$ vs DPS	0.04	0.06	0.04	0.03	0.04	0.01

Table 2. Correlation parameters $\mathcal{P}_{ij}^a$. Numbers shown in bold signals that corresponding kinematical distribution can be potentially used to discriminate two corresponding channels.

state. For example, for $J/\psi\chi_c$ leading order processes are forbidden completely. By switching the final state one can also turn on or off different sets of the underlying Feynman diagrams.

At the hadronic level we have calculated cross section and various differential distributions for $J/\psi J/\psi$ and $\chi_c J/\psi$ pair production at LHCb, $\sqrt{s} = 13\,\text{TeV}$. The effect of double parton scattering mechanism was also estimated. In the talk it was shown that azimuthal and $|\Delta y$ asymmetries are most suitable to separate different kinds of contributions.

In our future work we are going to consider different polarization asymmetries in NLO $J/\psi J/\psi$ and $\chi_c J/\psi$ production.

More detailed description of the discussed processes can be found in [20]. The author would like to thank coauthors of this paper A.K. Likhoded and S.V. Poslavsky. I would also like to thank I. Belyaev for fruitful discussions. The work was financially supported by he Russian Foundation of Basic Research grant #14-02-00096.

References

[1] S. P. Baranov and A. H. Rezaeian, Phys. Rev. **D93**, 114011 (2016), arXiv:1511.04089[hep-ph].
[2] A. K. Likhoded, A. V. Luchinsky, and S. V. Poslavsky, Phys. Rev. **D86**, 074027 (2012), arXiv:1203.4893[hep-ph].
[3] A. K. Likhoded, A. V. Luchinsky, and S. V. Poslavsky, Phys. Rev. **D90**, 074021 (2014), erXiv:1409.0693[hep-ph].
[4] R. Aaij et al. (LHCb), Phys. Lett. **B707**, 52 (2012), arXiv:1109.0963[hep-ex].
[5] V. M. Abazov et al. (D0), Phys. Rev. **D90**, 111101 (2014), arXiv:1406.2380[hep-ex].
[6] P. Ronchese, in *12th Conference on the Intersections of Particle and Nuclear Physics (CIPANP 2015) Vail, Colorado, USA, May 19-24, 2015* (2015), arXiv:1509.09276[hep-ex], URL http://inspirehep.net/record/1395464/files/arXiv:1509.09276.pdf.
[7] C. Collaboration (CMS) (2016).
[8] V. G. Kartvelishvili and S. M. Esakiya, Yad. Fiz. **38**, 722 (1983).
[9] B. Humpert and P. Mery, Z. Phys. **C20**, 83 (1983).
[10] A. V. Berezhnoy, A. K. Likhoded, A. V. Luchinsky, and A. A. Novoselov, Phys. Rev. **D84**, 094023 (2011), arXiv:1101.5881[hep-ph].
[11] J.-P. Lansberg and H.-S. Shao, Phys. Rev. Lett. **111**, 122001 (2013), arXiv:1308.0474[hep-ph].
[12] J.-P. Lansberg and H.-S. Shao, Phys. Lett. **B751**, 479 (2015), arXiv:1410.8822[hep-ph].
[13] L.-P. Sun, H. Han, and K.-T. Chao (2014), arXiv:1404.4042[hep-ph].
[14] G. T. Bodwin, E. Braaten, and G. P. Lepage, Phys. Rev. **D51**, 1125 (1995), [Erratum: Phys. Rev.D55,5853(1997)], hep-ph/9407339.
[15] E. Braaten and J. Lee, Phys. Rev. **D67**, 054007 (2003), [Erratum: Phys. Rev.D72,099901(2005)], hep-ph/0211085.
[16] S. Dulat, T.-J. Hou, J. Gao, M. Guzzi, J. Huston, P. Nadolsky, J. Pumplin, C. Schmidt, D. Stump, and C. P. Yuan, Phys. Rev. **D93**, 033006 (2016), arXiv:1506.07443[hep-ph].
[17] H.-L. Lai, M. Guzzi, J. Huston, Z. Li, P. M. Nadolsky, J. Pumplin, and C. P. Yuan, Phys. Rev. **D82**, 074024 (2010), arXiv:1007.2241[hep-ph].
[18] R. Aaij et al. (LHCb), JHEP **10**, 172 (2015a), arXiv:1509.00771[hep-ex].
[19] R. Aaij et al. (LHCb) (2015b), arXiv:1510.05949[hep-ex].

[20] A. K. Likhoded, A. V. Luchinsky and S. V. Poslavsky, Phys. Rev. D **94**, no. 5, 054017 (2016) [arXiv:1606.06767 [hep-ph]].